Title	Exploring common control principles underlying versatile body-limb coordination in many-legged locomotion
Author(s)	Yasui, Kotaro; Seino, Genta; Yamaichi, Tatsumi et al.
Citation	The 11th International Symposium on Adaptive Motion of Animals and Machines (AMAM2023). 2023, p. 51-52
Version Type	VoR
URL	https://doi.org/10.18910/92262
rights	
Note	

Exploring common control principles underlying versatile body–limb coordination in many-legged locomotion

Kotaro Yasui[1,2], Genta Seino[2,3], Tatsumi Yamaichi[2,3], Yusei Sugiyama[2,3], Takeshi Kano[2], Akio Ishiguro[2]

[1]Frontier Research Institute for Interdisciplinary Sciences, Tohoku University, Japan

[2]Research Institute of Electrical Communication, Tohoku University, Japan

[3]Department of Electrical Engineering, Graduate School of Engineering, Tohoku University, Japan

k.yasui@riec.tohoku.ac.jp

1 Introduction

Many-legged animals, such as centipedes and millipedes, can walk effectively by coordinating their body and limb motions. Such body–limb coordination patterns differ depending on the species and locomotor speed [1]. For example, house centipedes and millipedes move by propagating a posterior–anterior wave of leg movements, called a direct-wave gait, with little body undulation. By contrast, certain species of centipedes (e.g., *Scolopendra subspinipes mutilans*) locomote by propagating an anterior-posterior wave of leg movements, called a retrograde-wave gait, and they additionally employ a wave of trunk movement coordinated with the leg movements as their locomotion speed increases [2].

Thus, it is essential to determine whether certain common control principles underly the various body–limb coordination patterns in many-legged locomotion. Understanding such control principles would facilitate the design of simple and functional controllers for multi-legged robots and deepen our understanding of biological locomotor circuits in animals. Previous studies that focused on the coordination patterns between legs proposed mathematical models that could reproduce one or multiple specific gaits of myriapods in simulations and robots [3–5]. However, the essential control principle that explains the versatile locomotor patterns, including body–limb coordination, remains unclear.

To address this issue, we reconsidered the coordination mechanism of the trunk and limbs for effective propulsion from a physical viewpoint and proposed simple decentralized control mechanisms for the local body segment. Preliminary simulation results indicated that our single control principle could explain two distinct body–limb coordination patterns: direct-wave gait without body undulation and retrograde-wave gait with body undulation.

2 Model

2.1 Overview of the mechanical system

We constructed a two-dimensional physical model of myriapods on a horizontal plane using a mass–spring–damper system (Fig. 1a). Each body segment
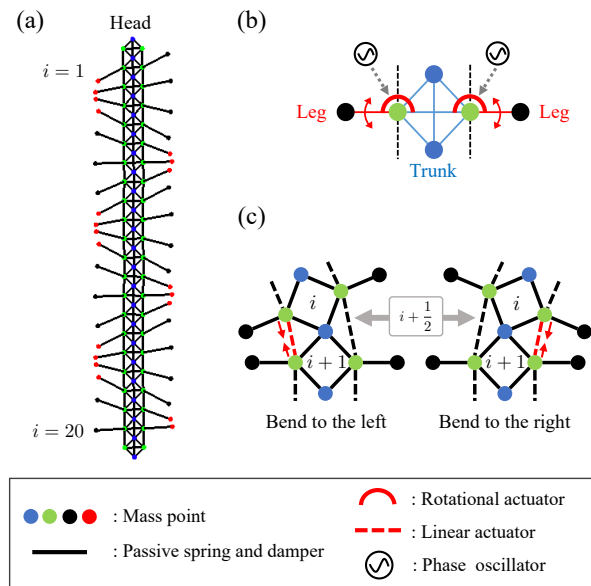

Figure 1: Schematic of the physical model: (a) overview of the body structure, (b) magnified view of a single body segment, and (c) linear actuators for body bending movement.

has a pair of legs, and the base is connected to the trunk with a rotational actuator to generate leg movement (Fig. 1b). The trunk is connected to the adjacent body segments via linear actuators implemented at the left and right sides of the body; this mechanism replicates the bending movement of the body (Fig. 1c).

The leg and body actuators generate torques and forces to achieve the target positions based on proportional-derivative control. Specifically, a phase oscillator was used for each leg (Fig. 1b), and the leg position was controlled according to the oscillator phase. The leg was assumed to be in the swing or stance phase when the oscillator phase was between 0 and π or between π and 2π. Dynamic frictional forces from the ground acted on the leg tips during the stance phase.

2.2 Proposed control principles

To understand the common control principle underlying the versatile body–limb coordination patterns in many-legged locomotion, we hypothesized the following: (1) During any gait, the trunk and limbs are in a coordinated mo-
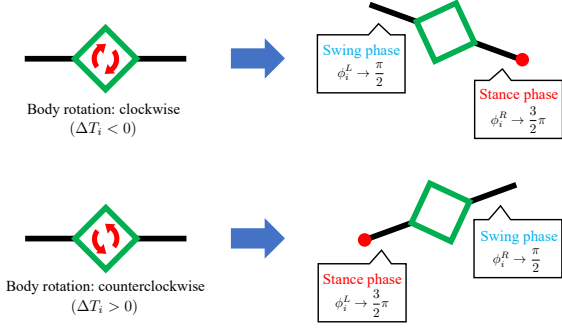
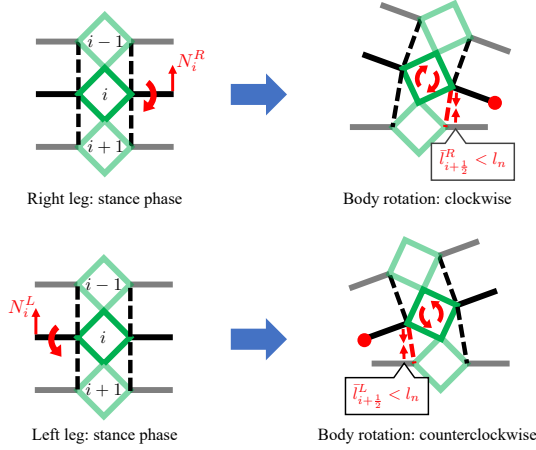**Figure 2:** Schematic of the sensory feedback from body to limb.

Figure 3: Schematic of the sensory feedback from limb to body.

tion to avoid losing the propulsive force obtained by the leg movement from the environment. (2) The body–limb coordination is established through bidirectional sensory feedback between the trunk and limbs. Here, we briefly explain the hypothesized control principles for the leg and body movements.

Leg control

The time evolution of the oscillator phase for the right (ϕ_i^R) and left legs (ϕ_i^L) is determined as follows:

$$\dot{\phi}_i^R = \omega + \sigma_T \Delta T_i \cos \phi_i^R, \tag{1}$$
$$\dot{\phi}_i^L = \omega - \sigma_T \Delta T_i \cos \phi_i^L, \tag{2}$$

where ω denotes the intrinsic angular velocity, σ_T denotes the positive constant, and ΔT_i denotes the rotational force acting on the ith body trunk. The second terms on the right side of Eqs. (1) and (2) represent the proposed sensory feedback. As shown in Fig. 2, when the trunk rotates in the clockwise direction ($\Delta T_i < 0$), the sensory feedback causes the right leg to stay in the stance phase ($\phi_i^R \to \frac{3\pi}{2}$), whereas the left leg tends to stay in the swing phase ($\phi_i^L \to \frac{\pi}{2}$). Thus, this sensory feedback enables the local body segment to effectively propel itself forward.

Body control

The target length of the $(i + \frac{1}{2})$th linear actuator ($\bar{l}_{i+\frac{1}{2}}^P$) is determined as follows (The suffix 'P' denotes the left or right side of the body):

$$\bar{l}_{i+\frac{1}{2}}^P = l_n - \beta \max[0, \tanh(\gamma N_i^P)], \tag{3}$$

where l_n is the natural length, β and γ are the positive constants, and N_i^P denotes the frictional force detected at the
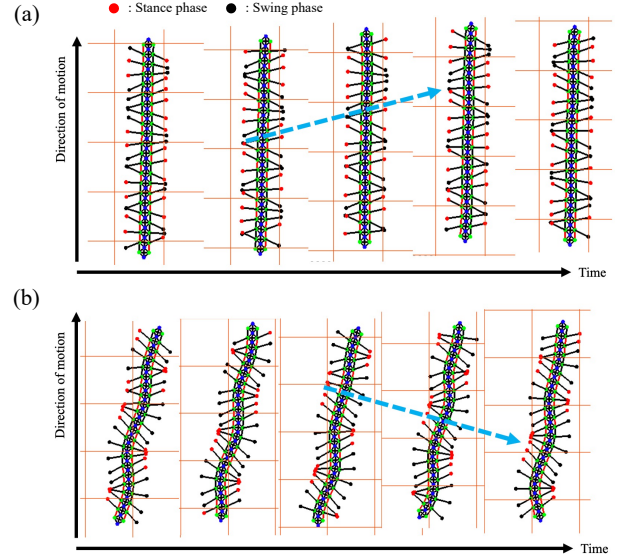

Figure 4: Simulation results: (a) $\beta = 1.7 \times 10^{-4}$[m], (b) $\beta = 1.7 \times 10^{-3}$[m]. The blue arrows indicate the propagation of the leg waves.

ith leg tip. Equation (3) indicates that the ipsilateral linear actuator immediately below the leg base contracts when the leg detects propulsive friction ($N_i^P > 0$) (Fig. 3). Thus, this sensory feedback can cause trunk rotation in the effective direction for propulsion.

3 Simulation results

To test our proposed model, we first performed simulations using different values of β, the magnitudes of the limb-to-body feedback, and observed the locomotor patterns that emerged. The other parameter values were as follows: $\omega = 25.0$[s^{-1}], $\sigma_T = 2.7 \times 10^3$[kg^{-1}m^{-1}s], $l_n = 6.8 \times 10^{-3}$[m], $\gamma = 5.0 \times 10^{-1}$. All the oscillator phases of the legs were set randomly in the initial condition. As shown in Fig. 4, a direct-wave gait with little body undulation emerges when β is small ($\beta = 1.7 \times 10^{-4}$[m]), whereas a retrograde-wave gait with body undulation emerges when β is large ($\beta = 1.7 \times 10^{-3}$[m]). Thus, the proposed control principle could generate two distinct body–limb coordination patterns. In the future, we will investigate whether other body–limb coordination patterns can be reproduced using different control parameters.

References

[1] Manton, S, M., The Arthropoda: Habits, Functional Morphology and Evolution. Clarendon Press, 1977.

[2] Anderson, B. D., Shultz, J. W. and Jayne, B. C., Axial kinematics and muscle activity during terrestrial locomotion of the centipede Scolopendra heros. *J. Exp. Biol.* 198, 1185–1195, 1995.

[3] Kano, T. et al., Decentralized control mechanism underlying interlimb coordination of millipedes, *Bioinspir. Biomim.*, 12, 036007, 2017.

[4] Ambe, Y. et al., Generation of Direct-, Retrograde-, and Source-Wave Gaits in Multi-Legged Locomotion in a Decentralized Manner via Embodied Sensorimotor Interaction. *Frontiers in neural circuits*, 15, 2021.

[5] Yasui, K. et al., Adaptive centipede walking via synergetic coupling between decentralized control and flexible body dynamics, *Front. Robot. AI*, 9, 797566, 2022.